

Modelling background charge rearrangements near single-electron transistors as a Poisson process

HEINZ-OLAF MÜLLER^{1,2(*)}, MIHA FURLAN^{1,3}, THOMAS HEINZEL¹ and KLAUS ENSSLIN¹

¹ *Solid-State Physics Laboratory, ETH Zürich – CH-8093 Zürich, Switzerland*

² *Integrated Systems Engineering, ISE – CH-8008 Zürich, Switzerland*

³ *Swiss Federal Office of Metrology and Accreditation, metas – CH-3003 Bern-Wabern, Switzerland*

PACS. 73.23.Hk – Coulomb blockade; single-electron tunnelling.

PACS. 73.50.Gr – Charge carriers: generation, recombination, lifetime, trapping, mean free paths.

PACS. 02.50.Ey – Stochastic processes.

Abstract. – Background charge rearrangements in metallic single-electron transistors are modelled in two-level tunnelling systems as a Poisson process with a scale parameter as only variable. The model explains the recent observation of asymmetric Coulomb blockade peak spacing distributions in metallic single-electron transistors. From the scale parameter we estimate the average size of the tunnelling systems, their density of states, and the height of their energy barrier. We conclude that the observed background charge rearrangements predominantly take place in the substrate of the single-electron transistor.

Introduction. – The metallic single-electron transistor (SET) [1, 2] is a possible building block of future electronics, based upon the controlled transfer of individual charges onto and off small isolated electrodes, called islands. However, due to the extreme sensitivity of SETs to charges close to these islands, a static background charge arrangement is essential for proper device operation [3, 4]. On the other hand, this very high sensitivity makes the SET an excellent device to investigate background charge rearrangements, *e.g.* in nearby two-level tunnelling systems (TLTS) [5, 6]. One issue of this paper is to determine the location of TLTSs within the device.

In recent experiments [7, 8] on Al/AlO_x/Al SETs it was shown that the distribution of nearest-neighbour spacings (NNS) between Coulomb blockade oscillation peaks is influenced by such charge rearrangements: they generate a pronounced tail in the NNS distribution towards smaller spacings (see left inset of fig. 1). Here, we propose a quantitative model for this tail. We argue that background charge rearrangements can be interpreted in terms of a Poisson process. This way, we can fit the shape of the NNS distribution tail, with a single scale parameter. From this fit, we find an average hopping distance in the TLTS of about 4 nm and conclude that the charge rearrangements do not occur in the tunnel barriers of the SET.

(*) hom@ise.ch

We can furthermore estimate the density of states of TLTSs and the barrier height between the two TLTS states.

Experimental observations and statistical model. – The NNS distribution $p(\Delta V_g)$ in fig. 1 is strongly peaked at $\Delta V_g = e/C_g$, but displays a remarkable tail towards lower ΔV_g as well, which contains up to one third of the total data points. Here, V_g and C_g denote the gate voltage and the gate capacitance, respectively. The spacings observed in the low- ΔV_g tail are stable: repeated and reversed gate voltage sweeps reveal the same statistical distribution of events. It has been attributed to the rearrangement of background charges in TLTSs [9], fig. 2a). A further important experimental result is that the NNS distribution does not depend on V_g : it was found [8] that the standard deviation of the n -th neighbour Coulomb peak spacings is proportional to \sqrt{n} .

The clearly observed hysteresis of the Coulomb peak pattern when reversing the gate scan direction [8] suggests the existence of metastable configurations, which explains the high stability and reproducibility of the experimental results. Neither the Coulomb blockade peak positions nor the underlying smooth $1/f$ noise spectrum depend on V_g or the scan speed. Hence, other excitations which could spontaneously flip a TLTS (like thermal activation) are much weaker compared to the parameters which we control in the experiment. Note that these experiments are different from dynamic and frequency dependent background charge noise measurements [5, 6, 10–12].

The focus of our model lies on the $p(\Delta V_g)$ distribution generated by TLTS fluctuations. Since the ΔV_g distribution is stable, a single sweep of V_g already reveals it completely. Therefore, our study is restricted to a single gate sweep. During this sweep, the electric field around the island electrode retains its direction thus causing all background charges in TLTSs to ‘hop’ either towards or away from the island electrode. Therefore, the total amount of charge Q_i influenced on the island is monotonic as a function of V_g and is tested periodically (with respect to V_g) by the position of the Coulomb peak. Background charges in TLTSs contribute to the variation of ΔV_g by influencing additional charge on the central island.

We display the situation of the experiment in fig. 2 schematically. While sweeping V_g , TLTS switching events lead to stochastic jumps of the island charge Q_i , see fig. 2b). Due to the discrete technique of measuring the Coulomb spacings, the Q_i jumps are recorded at almost regular V_g intervals. From a mathematical point of view, we can consider V_g as a function of Q_i just as well. In this picture, see fig. 2c), we observe steps of V_g of (almost) uniform height ΔV_g which occur at arbitrary values of Q_i .

The sequence of Q_i values, at which V_g jumps, forms a stochastic process where the charge Q_i takes over the role of the time in the common notation of stochastic processes. Assuming statistic independence of the jumps (see below), the process can be identified as Poisson process [13]. The single requirement for a Poisson process is the independence of the individual events. The process is described by a single scale parameter $1/\gamma$. The probability that n jumps occur before the charge Q_i is accumulated on the island, is given by [13]

$$p_n(Q_i) = \frac{(\gamma Q_i)^n}{n!} \exp(-\gamma Q_i). \quad (1)$$

The Poisson process is non-stationary, which in our context corresponds to an average number of jumps $\langle n \rangle = \gamma Q_i$, which depends on Q_i . γQ_i also corresponds to the square standard deviation, *i.e.* $\langle \langle n \rangle \rangle = \langle n^2 \rangle - \langle n \rangle^2 = \gamma Q_i$.

In the framework of the Poisson process it is possible to describe the tail of the $p(\Delta V_g)$ distribution function. For that purpose we transform $p(\Delta V_g)$ into $p(\Delta Q_i)$, which follows from

$$\Delta Q_i = e - \Delta V_g C_g. \quad (2)$$

$p(\Delta Q_i)$ is peaked at $\Delta Q_i = 0$ and displays a tail into the positive, see right inset in fig. 1. The probability distribution of the charge difference ΔQ_i between two jumps corresponds to the waiting time distribution of the conventional Poisson process. Therefore

$$p(\Delta Q_i) = -\frac{dp_0(\Delta Q_i)}{d\Delta Q_i} = \gamma \exp(-\gamma \Delta Q_i) \quad (3)$$

is the tail of the distribution function $p(\Delta Q_i)$ with $p_0(\Delta Q_i)$ as defined in eq. (1). Finally, the mean value and square standard deviation of ΔQ_i also follow from the distribution function $p(\Delta Q_i)$:

$$\langle \Delta Q_i \rangle = \sqrt{\langle \langle \Delta Q_i \rangle \rangle} = \frac{1}{\gamma}. \quad (4)$$

Discussion. – It has to be noted that the presented stochastic model is only valid for the description of the tail of the $p(\Delta Q_i)$ distribution, but not its maximum. While the tail is due to events arising from randomly distributed TLTSs, for which the presumptions of the Poisson process will be proven to hold, the maximum reflects the regularly spaced Coulomb blockade peaks and is deterministic in nature. Fortunately, these two ranges can easily be distinguished in our experimental data (see fig. 1). In order to separate both domains, a phenomenological cut is made at $\Delta Q_{i,\min} = 0.01 e$, which corresponds via (2) to $\Delta V_{g,\max} = 0.99 e/C_g$.

Our model provides us with three independent methods of determining the value of its sole parameter $1/\gamma$: (i) a fit to eq. (3), (ii) the average $\langle \Delta Q_i \rangle$, and (iii) the deviation $\langle \langle \Delta Q_i \rangle \rangle$ according to eq. (4). For the data presented in fig. 1 we find the respective values: (i) $1/\gamma = (0.046 \pm 0.002) e$, (ii) $1/\gamma = 0.057 e$, and (iii) $1/\gamma = 0.043 e$. The discrepancy between the average obtained from (ii) and the other values can be shown to be due to the $\Delta Q_{i,\min}$ cutoff. However, the correspondence between (i) and (iii) is sufficient to demonstrate that the TLTS events are statistically independent because it reflects a unique feature of the Poisson process. This process provides an adequate description of $p(\Delta Q_i)$ and in turn $p(\Delta V_g)$. Measurements on five different SET devices of equal geometry and on the same substrate result in a mean $1/\bar{\gamma} = (0.047 \pm 0.003) e$.

The value of $1/\gamma$ provides a charge scale of the influence of TLTSs on the island charge Q_i . Thus, it describes the material properties and consequences of the sample manufacture. A small value of $1/\gamma$ corresponds to a short tail of the distribution functions $p(\Delta Q_i)$ and $p(\Delta V_g)$, which in turn correlates with few TLTS transitions per e/C_g interval and, thus, rather stable device operation. $1/\gamma$ also scales with device dimensions, as will be shown below.

A simple geometric argument allows us to deduce a mean tunnelling distance δ of the TLTS from $1/\gamma$. It is based on the “constant capacitance model” [14]: charge rearrangements within TLTSs induce potential shifts only, but they do not alter any capacitances. This is appropriate here, since only metal electrodes with high electron density and individual charges at the TLTS sites are considered. The assumption of constant capacitances is also supported by the experimental data, since the peak position of $p(\Delta V_g)$ is independent of V_g and the bias voltage (see figs. 1*d*) and 3*b*) in ref. [7], respectively). In addition, screening of the single TLTS charges is neglected, which is reasonable considering the low concentration of quasi-free electrons around them, *i.e.* in silicon oxide or aluminum oxide. The treatment is simplified by assuming a constant field between gate and island, and by assuming that only one electron is rearranged in a TLTS switching event.

In this case, Green's reciprocity theorem [15] can be applied to the setup displayed in fig. 2a),

$$\sum_{j=1}^n Q_j V'_j = \sum_{j=1}^n Q'_j V_j, \quad (5)$$

where $\{Q_j\}$ and $\{Q'_j\}$ are two charge configurations in a system of conductors and $\{V_j\}$ and $\{V'_j\}$ are the respective voltage configurations.

$\{Q_j\}$ shall be the charge configuration before and $\{Q'_j\}$ that after charge transfer. The influence on the gate electrode is negligible, *i.e.* $Q_1 = Q'_1$ and $V_1 = V'_1 = V_g$. Furthermore, we use a single charged TLTS,

$$Q_2 = e \quad Q'_2 = 0 \quad Q_3 = 0 \quad Q'_3 = e.$$

In our model the charge on the island is conserved, $Q_4 = Q'_4 = Q_i$. The island potential, however, shows a slight increase, $V'_4 = V_4 + \Delta V_4$. This yields with eq. (5)

$$\Delta V_4 = \frac{e}{Q_i} (V_3 - V'_2). \quad (6)$$

For symmetry reasons the mutual contributions to the potentials V_3 and V'_2 cancel and $(V_3 - V'_2)$ is solely determined by V_g ,

$$V_3 - V'_2 = \frac{\delta}{D} V_g \quad (7)$$

using the gate-island separation D and the TLTS size δ (see fig. 2a)). In general, eq. (7) looks different for a different electrode geometry, but a characteristic length scale corresponding to D can be found and a similar formula will hold in most cases. The equation gives an upper estimate of the voltage difference since it assumes the TLTS to live in the high-field region. This region experiences the widest energy range of TLTS transitions and thus contributes most events to the statistics.

Finally, $Q_i = C_g V_g$ together with (6) and (7) yields

$$\Delta V_4 = \frac{\delta}{D} \frac{e}{C_g}. \quad (8)$$

This value is independent of V_g , as found in the experiment, due to the cancellation of the linear V_g dependence of Q_i and $(V_3 - V'_2)$.

Fixed capacitances allow us to relate ΔV_4 of eq. (8) to ΔV_g of eq. (2) and to establish a link between $1/\gamma$ of (3) and δ of (8). Given the regular Coulomb peak separation e/C_g , the link is provided by

$$\frac{\Delta V_4}{e/C_g} = \frac{1/\gamma}{e} \quad \delta = \frac{D}{e\gamma}. \quad (9)$$

Hence, γ scales linearly with D , *i.e.* the NNS tail is experimentally observable only for sufficiently small D . However, the result (9) is independent of the distance between the TLTS and the island. This is due to the assumption that the charge of the TLTS influences an equal amount of charge on the island, no matter what the capacitance (and thus the distance) between them is. In other words, this result follows directly from using the "constant capacitance model" and neglecting screening. Although ref. [8] discusses the TLTS influence in terms of a general model where the potential rather than the charge of a TLTS is kept fixed, producing both a distance and a size dependence of the TLTSs, it is not in contradiction to

the present treatment. We rather consider the range of small charge displacement and small distance from the SET island here (top left part of fig. 5*b*) in ref. [8]). These conditions are reasonable and have already been concluded in [7, 8]. Both methods yield corresponding results in case of short TLTS–island distance.

The values obtained for $1/\gamma$ easily translate into a characteristic tunnelling distance δ within TLTSs, using eq. (9). With $D = 70 \dots 100$ nm, depending on the device, we obtain $\delta = (3.94 \pm 0.19)$ nm, taking into account eight experiments with geometrically *different* SETs measured at 10 mK. This value agrees well with other experiments [6–8, 16].

The value we extract for δ thus exceeds the thickness of the SET tunnel barriers, which is typically 2 nm or less. Hence the monitored trap states cannot reside in a tunnel junction itself, but must be located in the surface oxide or the substrate [6]. The measurements [7, 8] suggest the tunnelling processes themselves not to be field–assisted, since the probability of a TLTS event does not depend on V_g . Under these circumstances $\delta \approx 4$ nm is a rather large value. In the case of tunnelling between trap states, however, the larger tunnelling distance can be compensated by lower barrier height, which can in fact be well below 1 eV and still warrant electric field independence of the tunnelling process. Thus, the height of the energy barrier between the two TLTS sites is limited towards low energies by the maximum potential difference (≈ 80 meV) and towards high energies by the necessary barrier transparency (≈ 0.7 eV). The neglect of multiple electron transitions within one TLTS in our model might be another reason for the large value of δ .

Information on TLTS switching events at elevated temperatures is hard to access due to the increasing overlap between the main peak of the $p(\Delta Q_i)$ distribution and its tail, as the temperature increases. Measurements performed at temperatures up to 200 mK did not reveal any significant variation of $1/\gamma$.

The determination of $1/\gamma$ (and δ) also provides an estimate of the density of states of the TLTSs. The data presented in fig. 1 contain 572 Coulomb oscillation periods, 177 of which belong to the tail of $p(\Delta V_g)$. While the total energy range scanned by V_g is $572 e/C_g \approx 1.8$ V, the potential shift experienced between the two states of a TLTS is only δ/D times this value. Hence, the average density of states is

$$D_{\text{TLTS}} = \frac{177}{572} \frac{D}{\delta} \frac{C_g}{e^2} \approx 2.1 \frac{1}{\text{meV}}.$$

Owing to lacking information on the energy level of the whole TLTS and its inner structure (which might allow, for instance, more than one TLTS transition), D_{TLTS} does not easily translate into a density of states of the traps accommodating the TLTS.

Defects with internal degrees of freedom can switch between metastable configurations also due to their interaction with a thermal bath or by photon excitations. Low–frequency excess noise even in high–quality devices is significantly generated by dynamic fluctuations of such defects [16]. While a single fluctuator, also known as random telegraph fluctuator (RTF), shows a Lorentzian spectrum, an ensemble of RTF results in the typical $1/f$ noise [17]. It is reasonable and tempting to assume that the TLTS effects investigated in our studies are of the same origin as RTF generated noise. Due to the metastable nature of the TLTS, the dynamics of a fluctuator crucially depend on its energy threshold separation. However, this is only vaguely known from our experiments via the observation of Coulomb peak pattern hysteresis [8]. Furthermore, it is not clear how to extrapolate the data, where we can resolve TLTS events with a large hysteresis, towards a small energy interval of $k_B T$, *i.e.* for fluctuators of small time constants contributing to non-zero frequency noise. Therefore, a decisive conclusion on consequences of our results for dynamic fluctuations and noise is too speculative at the moment. However, his subject is under further investigation.

Conclusion. – We have investigated charge transfer in two-level tunnelling systems (TLTSs). The study is based on measurements performed on metallic SETs. The charge transfer can be described in terms of a Poisson process, where the influenced charge Q_i replaces the usual time variable. Thus, the prominent tail of the probability distribution function $p(\Delta V_g)$ is governed by a single scale parameter $1/\gamma$. We can associate this parameter with a length scale δ of the TLTS. We find $\delta = (3.94 \pm 0.19)$ nm for the samples of different geometries under consideration. From this result we conclude that the SET tunnel barriers are in our case free of TLTSs. The fluctuators reside in the oxide around the island electrode or in the substrate. The height of the energy barrier separating two TLTS states is between 80 meV and 0.7 eV and the density of states of TLTS is found to be $2.1 (\text{meV})^{-1}$.

* * *

We are indebted to Sergey V. Lotkhov for the excellent sample manufacture, as well as to Mathias Wagner and Ulrich Zülicke for thorough reading of the manuscript.

REFERENCES

- [1] FULTON T. A. and DOLAN G. J., *Phys. Rev. Lett.*, **59** (1987) 109.
- [2] *Single Charge Tunneling: Coulomb Blockade Phenomena in Nanostructures*, edited by GRABERT H. and DEVORET M. H., NATO ASI Series B, (Plenum, New York), Vol. **294**, 1992.
- [3] KOROTKOV A. N., *Phys. Rev. B*, **49** (1994) 10381.
- [4] COVINGTON M., KELLER M. W., KAUTZ R. L. and MARTINIS J. M., *Phys. Rev. Lett.*, **84** (2000) 5192.
- [5] ZIMMERLI G., EILES T. M., KAUTZ R. L. and MARTINIS J. M., *Appl. Phys. Lett.*, **61** (1992) 237.
- [6] ZORIN A. B., AHLERS F.-J., NIEMEYER J., WEIMANN T., WOLF H., KRUPENIN V. A. and LOTKHOV S. V., *Phys. Rev. B*, **53** (1996) 13682.
- [7] FURLAN M., HEINZEL T., JEANNERET B., LOTKHOV S. V. and ENSSLIN K., *Europhys. Lett.*, **49** (2000) 369.
- [8] FURLAN M., HEINZEL T., JEANNERET B. and LOTKHOV S. V., *J. Low Temp. Phys.*, **118** (2000) 297.
- [9] LANDAUER R., *J. Appl. Phys.*, **33** (1962) 2209.
- [10] TAVKHELIDZE A. N. and MYGIND J., *J. Appl. Phys.*, **83** (1998) 310.
- [11] KENYON M., COBB J. L., AMAR A., SONG D., ZIMMERMAN N. M., LOBB C. J. and WELLSTOOD F. C., *IEEE Trans. Appl. Supercond.*, **9** (1999) 4261.
- [12] FUJISAWA T. and HIRAYAMA Y., *Appl. Phys. Lett.*, **77** (2000) 543.
- [13] VAN KAMPEN N. G., *Stochastic Processes in Physics and Chemistry* (Elsevier, Amsterdam) 1981.
- [14] KOUWENHOVEN L. P., MARCUS C. M., MCEUEN P. L., TARUCHA S., WESTERVELT R. M. and WINGREEN N. S., in *Mesoscopic Electron Transport*, edited by SOHN L. L., KOUWENHOVEN L. P. and SCHÖN G., NATO ASI Series E, (Kluwer, Dordrecht), Vol. **345**, 1997, p. 105–214.
- [15] SMYTHE W. R., *Static and Dynamic Electricity* (McGraw–Hill, New York) 1968.
- [16] For a review, see e.g.: KIRTON M. J. and UREN M. J., *Adv. Phys.*, **38** (1989) 367.
- [17] DUTTA P. and HORN P. M., *Rev. Mod. Phys.*, **53** (1981) 497.

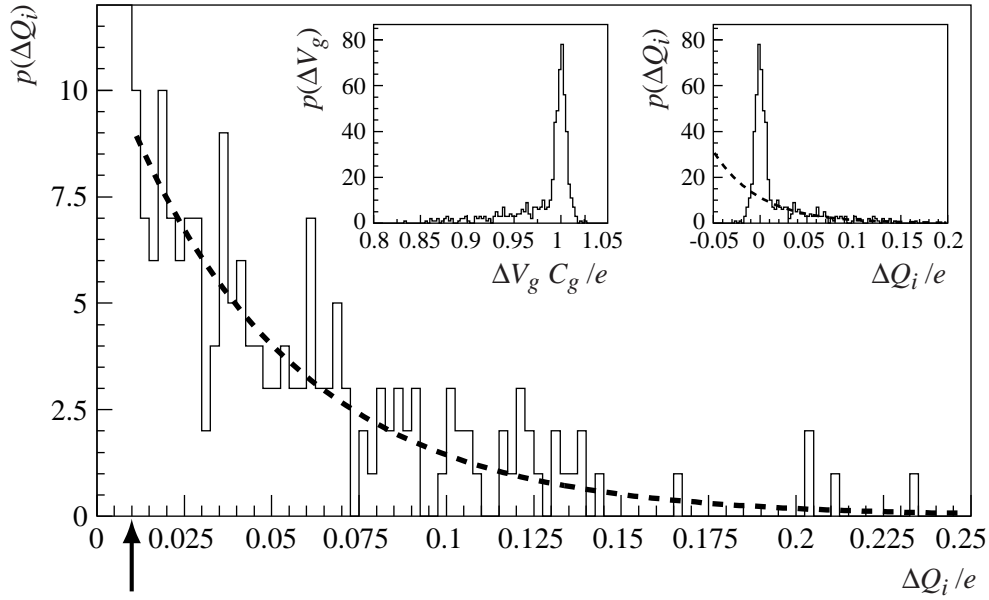


Fig. 1 – Determination of $1/\gamma$ from a fit to experimental data. Equation (3) is used to fit the tail of the probability distribution function $p(\Delta Q_i)$. The main plot is enlarged to emphasize the fit of the tail, whereas the left and right inset show the complete $p(\Delta V_g)$ and $p(\Delta Q_i)$ histograms, respectively. The dashed lines in the plots represent the fit, and the arrow indicates the limit of the fit range.

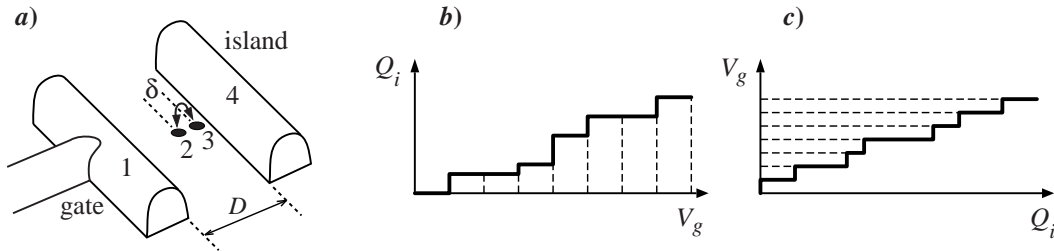


Fig. 2 – Background charges in two-level tunnelling systems. *a*) Schematic drawing of the SET's gate (1) and island (4) electrode, which are separated by the distance D . Because the island is quasi-isolated, the source-drain electrodes are not considered for electrostatic arguments. A TLTS is located between island and gate, where a charge can tunnel a distance δ from one site (2) to another (3) or vice versa. *b*) The island charge Q_i displays arbitrary jumps at definite values of V_g . *c*) Transition to uniform V_g steps at arbitrary Q_i values.